

Application of Hamilton variational principle for vibration of fluid filled structure

Khaled Mohamed Khedher^{*1}, Muzamal Hussain^{2,3}, Rizwan Munir⁴,
Saleh Alsulamy⁵ and Ayed Eid Alluqmani⁶

¹Department of Civil Engineering, College of Engineering, King Khalid University, Abha 61421, Saudi Arabia

²Department of Mathematics, University of Sahiwal, Sahiwal, Pakistan

³Department of Mathematics, Govt. College University Faisalabad, 38000, Faisalabad, Pakistan

⁴Department of statistics, jiangxi university of finance and economics, Nanchang city, Jiangxi province, China 330013

⁵Department of Architecture & Planning, College of Engineering, King Khalid University, Abha 61421, Saudi Arabia

⁶Department of Civil Engineering, Faculty of Engineering, Islamic University of Madinah, Saudi Arabia

(Received March 24, 2021, Revised August 10, 2023, Accepted August 14, 2023)

Abstract. Vibration investigation of fluid-filled three layered cylindrical shells is studied here. A cylindrical shell is immersed in a fluid which is a non-viscous one. Shell motion equations are framed first order shell theory due to Love. These equations are partial differential equations which are usually solved by approximate technique. Robust and efficient techniques are favored to get precise results. Employment of the wave propagation approach procedure gives birth to the shell frequency equation. Use of acoustic wave equation is done to incorporate the sound pressure produced in a fluid. Hankel's functions of second kind designate the fluid influence. Mathematically the integral form of the Lagrange energy functional is converted into a set of three partial differential equations. It is also exhibited that the effect of frequencies is investigated by varying the different layers with constituent material. The coupled frequencies changes with these layers according to the material formation of fluid-filled FG-CSs. Throughout the computation, it is observed that the frequency behavior for the boundary conditions follow as; clamped-clamped (C-C), simply supported-simply supported (SS-SS) frequency curves are higher than that of clamped-simply (C-S) curves. Expressions for modal displacement functions, the three unknown functions are supposed in such way that the axial, circumferential and time variables are separated by the product method. Computer software MATLAB codes are used to solve the frequency equation for extracting vibrations of fluid-filled.

Keywords: Hankel's functions; fluid-filled; MATLAB; strain energy; three layered

1. Introduction

Vibration fluid-filled shell problems occur in industrial engineering fields. Their vibration analysis predicts to approximate their experimental results. Nature of a shell material plays an important role in specifying their vibration frequencies. Stability of a cylindrical shell depends highly on these aspects of material. More the shell material sustains a load due to physical situations, the more the shell is stable.

During the recent years, study of submerged cylindrical shell has gained the attention of researchers doing work on their vibration characteristics. Advanced composite materials keep extreme particular stiffness, strength and are resistant to corrosion. More than one type of materials is used to structure the functionally graded materials and their physical properties. The acoustic wave equation is applied to extract influence of a fluid on shell vibrations. Firstly, Love (1888) presented the Kirchhoff's hypotheses for plates. After that this theory became a foundation stage for building new ones by changing physical terms expressions vary from one surface to the other surface. In these surfaces, one has highly heat resistance property while other may

preserve great dynamical perseverance and differs mechanically and physically in regular manner from one surface to other surface, making them of dual physical appearance. All these materials have changeable outer and inner sides and their physical properties greatly differ from each other (Suresh and Mortensen 1997, Koizumi 1997). These materials are organized by various techniques and their applications are seen in dynamical elements such as plates, beams and shells. Moreover, they are also observed in space crafts, nuclear reactors and missiles technology etc. Xiang *et al.* (2002) formed some closed form solution functions for studying vibrations of cylindrical shells. The mid-way ring supports were clamped around the shells. Sewall and Naumann (1968) considered the vibration analysis of CSs based on analytical and experimental methods. The shells were strengthened with longitudinal stiffeners. Chung *et al.* (1981) investigated the vibrations of fluid-filled CSs and presented an analysis of experimental and analytical investigation.

Jiang and Olson (1994) recommended the characteristics of analysis of stiffened shell using finite element method to diminish large computational efforts which are required in the conventional finite element analysis. Wang *et al.* (1997) scrutinized the vibrations of ring-stiffened CSs using Ritz polynomial functions. Materials of both shells and rings were of isotropic nature. These shells were stiffened with isotropic rings having three types of locations on the shell outer surface. To increase the stiffness of CSs was stabilized

*Corresponding author, Ph.D.,
E-mail: kkhedher@kku.edu.sa

by ring-stiffeners. Isotropic materials are the constituents of these rings. A large use of shell structures in practical applications makes their theoretical analysis an important field of structural dynamics. Any predicted fatigue due to burden of vibrations is evaded by estimating their dynamical aspects. Study of vibration characteristics of fluid-filled cylindrical shells is a widely area of research in applied mathematics and theoretical mechanics. Analytical investigation of vibrations of these shells are performed to estimate the probable dynamical response. Variations in the shell physical parameters are inducted to enhance their strength and stability. Addition of more physical parameters may give rise more instability in a system of a submerged cylindrical shell (CSs).

Variations of physical and material parameters. To elude any complications which may risk a physical system their analytical investigation was done. Sharma *et al.* (1998) determined frequencies of composite cylindrical shells containing fluid. They estimated the axial modal deformations by trigonometric functions. Amabili *et al.* (1999) assessed the free and forced non-linear vibrations of circular cylindrical shell with the quiescent, dense, inviscid and incompressible fluid. The analyses are made for the large moderately vibrations using Donnell's shallow-shell model. Also the dense fluid is studied for the influence of both the internal and external side of the shell. In the external side of the shell, the fluid was considered as an unbounded domain in the radial direction, while internally, the shell was considered as filled completely. Wang and Lai (2000) examined a novel approach for the evaluation of eigen - frequencies of cylindrical shells. The numerical process adopted by them was alike the wave propagation approach (WPA). Ergin and Temarel (2002) did a vibration study of cylindrical shells. The shells lied in a horizontal direction and contained fluid and submerged in it. Zhang (2002) studied vibrations of CSs submerged in a fluid. It was seen that the fluid factor impressed vibration shell frequencies to a significant limit. Najafizadeh and Isvandzibaei (2007) applied ring supports to CSs for vibration analysis of along the tangential direction and founded their research on angular deformation theory of higher order. The angular deformation was used for shell equations and determined the effects of constituent volume fractions and shell configurations on the shell vibrations. FG material parameters were changed step by step.

Shah *et al.* (2009) and Sofiyev and Avcar (2010) studied stability of CSs based on Rayleigh - Ritz and Galerkin technique using elastic foundations. The structures of cylindrical shell are tackled under the exponential law and axial load. Naeem *et al.* (2013) conducted the vibrational behavior of submerged FG-CSs. The problem of submerged cylindrical shells were frequently met where fluid envelopes a structure. The present problem consists of a cylindrical shell submerged in a fluid and surrounded by ring supports. There is no evidence found where this problem has not been studied earlier. Ansari *et al.* (2015) performed nonlocal model for the frequencies of multi-walled carbon nanotubes with small effects subject to various boundary conditions (BCs) using Rayleigh-Ritz technique. The governing equation was formulated based on Flügge's and nonlocal shell theory. Some new resonant

frequencies were identified with the association of vibrational modes and circumferential modes into shell model. Recently some researcher used different methods for nonlinear modeling (Eltaher *et al.* 2019, Ebrahimi *et al.* 2019, Safaei *et al.* 2019, Shahsavari *et al.* 2019, Benmansour *et al.* 2019, Ma, 2022, He *et al.* 2021, 2022, Jweeg *et al.* 2007, 2009, 2010).

According to our knowledge, up to now little is known about the vibration analyses of varying three layers in different configuration and have not been investigated for fluid-filled three layered FG-CS based on wave propagation approach. The proposed model are quite straightforward for the vibrational analysis of these structures of CSs. A large use of shell structures in practical applications makes their theoretical analysis an important field of structural dynamics. Since a shell problem is a physical one, so their vibrational behaviors are distorted by variations of physical and material parameters. It is also exhibited that the effect of frequencies by varying the different layers with constituent material. The coupled frequencies changes with these layers according to the material formation of fluid-filled FG-CSs. Throughout the computation, it is observed that the frequency behavior for the boundary conditions follow as, clamped-clamped (C-C), simply supported-simply supported (SS-SS) frequency curves are higher than that of clamped-simply (C-S) curves. Also the Love shell model based on the wave propagation approach for estimating fundamental natural frequency has been developed to converge more quickly than other methods and models. The presented vibration modeling and analysis of CSs may be helpful especially in applications such as oscillators and in non-destructive testing. To elude any complications which may risk a physical system their analytical investigation is done.

2. Functionally graded material

The modeling of FG-CS is due to mixing two or more than two materials like ceramic and metal and the distribution of various functions and properties (physical and material), is termed as rule of mixture. Power law function has been utilized for with particular index using material properties in the thickness direction. The temperature and properties variations have been obtained by using the property of temperature and volume fraction. The distributions of volume fraction for all types of CSs are assumed as (Chi and Chung 2006).

$$V_f = \left[\frac{z}{h} + \frac{1}{2} \right]^N \quad (1)$$

where N , h and z , respectively, denoted for power law index, thickness and the coordinate, where z which varies from zero to infinity. A FG-CS consisting of two constituent materials. In these types, nickel and stainless steel are used as the interior surfaces and the exterior surface respectively, but their arrangement has profound influence on the formation of FG-CSs. If E_1 and E_2 as Young's moduli, ν_1 and ν_2 as Poisson's ratios, ρ_1 and ρ_2 mass densities respectively. Then effective material quantities for FG material are

$$\begin{aligned}
 E_{FGM} &= [E_1 - E_2] \left[\frac{2z+h}{2h} \right]^N + E_2 \\
 \nu_{FGM} &= [\nu_1 - \nu_2] \left[\frac{2z+h}{2h} \right]^N + \nu_2 \\
 \rho_{FGM} &= [\rho_1 - \rho_2] \left[\frac{2z+h}{2h} \right]^N + \rho_2
 \end{aligned}
 \tag{2}$$

Touloukian *et al.* (1967) stated the material properties C at high temperature environ, with temperature-dependents which is a function of temperature. In Eq. (3), the constants ($C_0, C_{-1}, C_1, C_2, C_3$) are different for different material.

$$C = C_0 (C_{-1}T^{-1} + C_1T + C_2T^2 + C_3T^3)
 \tag{3}$$

At temperature 300K, for stainless steel and nickel, the material properties for FG-CS are: E, ν, ρ for stainless steel are $2.07788 \times 10^{11} \text{ N/m}^2, 0.317756$ and 8166 Kg/m^3 and nickel are $2.05098 \times 10^{11} \text{ N/m}^2, 0.3100$ and 8900 Kg/m^3 (Naeem *et al.* 2013).

3. Theoretical formation

Geometrical structure of a cylinder is sketched in Fig. 2. Strain energy U for FG-CS.

$$U = \frac{R}{2} \int_0^{L/2} \int_0^{2\pi} \{\alpha\}^T [S] \{\alpha\} d\theta dx
 \tag{4}$$

where

$$\{\alpha\}^T = \{e_1 \quad e_2 \quad \lambda \quad \kappa_1 \quad \kappa_2 \quad 2\tau\}
 \tag{5}$$

whereas (e_1, e_2, γ) and (k_1, k_2, τ) are referenced as surface curvature and surface strains.

$$[S] = \begin{bmatrix} A_{11} & A_{12} & 0 & B_{11} & B_{12} & 0 \\ A_{12} & A_{22} & 0 & B_{12} & B_{22} & 0 \\ 0 & 0 & A_{66} & 0 & 0 & B_{66} \\ B_{11} & B_{12} & 0 & D_{11} & D_{12} & 0 \\ B_{12} & B_{22} & 0 & D_{12} & D_{22} & 0 \\ 0 & 0 & B_{66} & 0 & 0 & D_{66} \end{bmatrix}
 \tag{6}$$

where the membrane (A_{ij}), coupling (B_{ij}) and flexural (D_{ij}) stiffness are expressed as:

$$\left. \begin{aligned}
 A_{ij} &= \int_{-\frac{h}{2}}^{\frac{h}{2}} Q_{ij} dz \\
 B_{ij} &= \int_{-\frac{h}{2}}^{\frac{h}{2}} z Q_{ij} dz \\
 D_{ij} &= \int_{-\frac{h}{2}}^{\frac{h}{2}} z^2 Q_{ij} dz
 \end{aligned} \right\}
 \tag{7}$$

The variation of stiffness moduli $A_{ij}, B_{ij}, D_{ij} \quad i, j = 1, 2, 6$ is modifies as:

$$\begin{aligned}
 A_{ij} &= A_{ij}^{in(Iso)} + A_{ij}^{m(FGM)} + A_{ij}^{ou(Iso)} \\
 B_{ij} &= B_{ij}^{in(Iso)} + B_{ij}^{m(FGM)} + B_{ij}^{ou(Iso)} \\
 D_{ij} &= D_{ij}^{in(Iso)} + D_{ij}^{m(FGM)} + D_{ij}^{ou(Iso)}
 \end{aligned}
 \tag{8}$$

The inner and outer layers are composed with isotropic material and middle one is with FG material of a cylindrical shell. For isotropic CSs the coupling stiffness B_{ij} condensed to zero when its material is isotropic and does not become zero when a cylindrical shell is structured from composite or laminated or functionally graded material.

Q_{ij} is reduced stiffness for isotropic materials with conjunction of E and ν are written as:

$$\left. \begin{aligned}
 Q_{11} &= Q_{22} = \frac{E}{1 - \nu^2} \\
 Q_{12} &= \frac{\nu E}{1 - \nu^2} \\
 Q_{66} &= \frac{E}{2(1 + \nu)}
 \end{aligned} \right\}
 \tag{9}$$

Strain energy modified form is achieved after putting $\{\alpha\}^T$ and $[S]$ in Eq. (4)

$$\begin{aligned}
 E_x &= -\frac{\partial \psi}{\partial x} = \frac{\partial \psi(x, y, t)}{\partial x} \cos\left(\frac{\pi z}{h}\right), \\
 H_x &= -\frac{\partial \phi}{\partial x} = \frac{\partial \phi(x, y, t)}{\partial x} \cos\left(\frac{\pi z}{h}\right), \\
 E_y &= -\frac{\partial \psi}{\partial y} = \frac{\partial \psi(x, y, t)}{\partial y} \cos\left(\frac{\pi z}{h}\right), \\
 H_y &= -\frac{\partial \phi}{\partial y} = \frac{\partial \phi(x, y, t)}{\partial y} \cos\left(\frac{\pi z}{h}\right), \\
 E_z &= -\frac{\partial \psi}{\partial z} = -\psi(x, y, t) \left(\frac{\pi}{h}\right) \sin\left(\frac{\pi z}{h}\right) - \frac{2z}{h} \psi_0, \\
 H_z &= -\frac{\partial \phi}{\partial z} = -\phi(x, y, t) \left(\frac{\pi}{h}\right) \sin\left(\frac{\pi z}{h}\right) - \frac{2z}{h} \phi_0,
 \end{aligned}
 \tag{10}$$

3.1 Relationship of strain-displacement expressions

With advancements in study of shell problem, new shell theories were developed and used to do vibration analysis of cylindrical shell problems. There found minute differences in numerical results when different shell theories were utilized. Applying Love shell theory, strain and curvature displacement expressions are stated as:

$$\{e_1, e_2, \gamma\} = \left\{ \frac{\partial u}{\partial x}, \frac{1}{R} \left(\frac{\partial v}{\partial \theta} + w \right), \left(\frac{\partial v}{\partial x} + \frac{1}{R} \frac{\partial u}{\partial \theta} \right) \right\}
 \tag{11}$$

$$\{k_1, k_2, \tau\} = \left\{ -\frac{\partial^2 w}{\partial x^2}, -\frac{1}{R^2} \left(\frac{\partial^2 w}{\partial \theta^2} - \frac{\partial v}{\partial \theta} \right), -\frac{1}{R} \left(\frac{\partial^2 w}{\partial x \partial \theta} - \frac{\partial v}{\partial x} \right) \right\}
 \tag{12}$$

On substitution of the expressions (11) and (12) in the relation (10), the strain energy U in modified form can be elaborated as

$$\begin{aligned}
 U &= \frac{R}{2} \int_0^L \int_0^{2\pi} \left[A_{11} \left(\frac{\partial u}{\partial x} \right)^2 + \frac{A_{22}}{R^2} \left(\frac{\partial v}{\partial \theta} - w \right)^2 \right. \\
 &\quad \left. + \frac{2A_{12}}{R} \left(\frac{\partial u}{\partial x} \right) \left(\frac{\partial v}{\partial \theta} - w \right) + A_{66} \left(\frac{\partial v}{\partial x} + \frac{1}{R} \frac{\partial u}{\partial \theta} \right)^2 \right]
 \end{aligned}
 \tag{13}$$

$$\begin{aligned}
& +2B_{11} \frac{\partial u}{\partial x} \frac{\partial^2 w}{\partial x^2} + \frac{2B_{12}}{R^2} \left(\frac{\partial^2 w}{\partial \theta^2} + w \right) \left(\frac{\partial u}{\partial x} \right) \\
& + \frac{2B_{12}}{R} \left(\frac{\partial^2 w}{\partial x^2} \right) \left(\frac{\partial v}{\partial \theta} - w \right) + \frac{2B_{22}}{R^3} \left(\frac{\partial v}{\partial \theta} - w \right) \left(\frac{\partial^2 w}{\partial \theta^2} + w \right) \\
& + B_{66} \left(\frac{\partial^2 w}{\partial x \partial \theta} + \frac{3}{4} \frac{\partial v}{\partial x} - \frac{1}{4R} \frac{\partial u}{\partial \theta} \right) \left(\frac{\partial v}{\partial x} + \frac{1}{R} \frac{\partial u}{\partial \theta} \right) \\
& + D_{11} \left(\frac{\partial^2 w}{\partial x^2} \right)^2 + \frac{D_{22}}{R^4} \left(\frac{\partial^2 w}{\partial \theta^2} + w \right)^2 + \frac{2D_{12}}{R^2} \frac{\partial^2 w}{\partial x^2} \left(\frac{\partial^2 w}{\partial \theta^2} + w \right) \\
& + 4D_{66} \left(\frac{\partial^2 w}{\partial x \partial \theta} + \frac{3}{4} \frac{\partial v}{\partial x} - \frac{1}{4R} \frac{\partial u}{\partial \theta} \right)^2] d\theta dx
\end{aligned}$$

Similarly kinetic energy for a CSs doing vibration is stated as

$$T = \frac{1}{2} \int_0^L \int_0^{2\pi} \rho_t \left[\left(\frac{\partial u}{\partial t} \right)^2 + \left(\frac{\partial v}{\partial t} \right)^2 + \left(\frac{\partial w}{\partial t} \right)^2 \right] R d\theta dx \quad (14)$$

The external work is defined as:

$$\delta \rho_t = \int_{-h/2}^{h/2} \rho dz \quad (15)$$

With the coalescence energies (strain and kinetic), the Lagrangian functional can be obtained can be given as (Sodel 1981).

$$\Pi = T - U \quad (16)$$

3.2 Shell dynamical equations

When a shell problem is formed in the integral form, it can be solved by applying the WPA. A cylindrical shell problem is described by a set of PDEs in which the three unknown functions represent the deformation displacement. These equations are framed from the Lagrangian functional with process of variation. So application of the Hamiltonian variational principle, the governing equations are given by:

$$\begin{aligned}
& R^2 A_{11} \frac{\partial^2 u}{\partial x^2} + \left(A_{66} - \frac{B_{66}}{R} + \frac{D_{66}}{4R^2} \right) \frac{\partial^2 u}{\partial \theta^2} + \\
& R \left(A_{12} + A_{66} + \frac{B_{12} + B_{66}}{R} - \frac{3D_{66}}{4R^2} \right) \frac{\partial^2 v}{\partial x \partial \theta} + R A_{12} \frac{\partial w}{\partial x} \\
& - \left(B_{12} + 2B_{66} - \frac{1}{R} D_{66} \right) \frac{\partial^3 w}{\partial x \partial \theta^2} - R^2 B_{11} \frac{\partial^3 w}{\partial x^3} = R^2 \rho_t \frac{\partial^2 u}{\partial t^2} \\
& R \left(A_{12} + A_{66} + \frac{B_{12} + B_{66}}{R} - \frac{3D_{66}}{R} \right) \frac{\partial^3 u}{\partial x \partial \theta} + \\
& \left(A_{22} + \frac{2B_{22}}{R} + \frac{D_{22}}{R^2} \right) \frac{\partial^2 v}{\partial \theta^2} + R^2 \left(A_{66} + \frac{3B_{66}}{R} + \frac{D_{66}}{4R^2} \right) \frac{\partial^2 v}{\partial x^2} \\
& + \left(A_{22} + \frac{B_{22}}{R} \right) \frac{\partial w}{\partial \theta} - \left(\frac{B_{22}}{R} + \frac{D_{22}}{R} \right) \frac{\partial^3 w}{\partial \theta^3} \\
& - R \left(B_{12} + 2B_{66} + \frac{D_{12} + 3D_{66}}{R} \right) \frac{\partial^3 w}{\partial x^2 \partial \theta} = R^2 \rho_t \left(\frac{\partial^2 v}{\partial t^2} + 2 \frac{\partial w}{\partial t} - v \right) \\
& - R A_{12} \frac{\partial u}{\partial x} + \left(B_{12} + 2B_{66} - \frac{D_{66}}{R} \right) \frac{\partial^3 u}{\partial x \partial \theta^2} + \\
& R^2 B_{11} \frac{\partial^3 u}{\partial x^3} - \left(A_{22} + \frac{B_{22}}{R} \right) \frac{\partial v}{\partial \theta} + \left(\frac{B_{22}}{R} + \frac{D_{22}}{R} \right) \frac{\partial^3 v}{\partial \theta^3} \\
& + R \left(B_{12} + 2B_{66} + \frac{D_{12} + 3D_{66}}{R} \right) \frac{\partial^3 v}{\partial x^2 \partial \theta} - A_{22} w
\end{aligned} \quad (17)$$

$$\begin{aligned}
& + \frac{2B_{22}}{R} \frac{\partial^2 w}{\partial \theta^2} - \frac{D_{22}}{R^2} \frac{\partial^4 w}{\partial \theta^4} - R^2 D_{11} \frac{\partial^4 w}{\partial x^4} - \\
& 2(D_{12} + 2D_{66}) \frac{\partial^4 w}{\partial x^2 \partial \theta^2} \\
& + 2RB_{12} \frac{\partial^2 w}{\partial x^2} = R^2 \rho_t \left(\frac{\partial^2 w}{\partial t^2} - 2 \frac{\partial v}{\partial t} - w \right)
\end{aligned}$$

After implicating the differential operator notations, a set of PDE is gained from Eq. (17):

$$\begin{aligned}
K_{11}u + K_{12}v + K_{13}w &= R^2 \rho_t \frac{\partial^2 u}{\partial t^2} \\
K_{21}u + K_{22}v + K_{23} &= R^2 \rho_t \left(\frac{\partial^2 v}{\partial t^2} + 2 \frac{\partial w}{\partial t} - v \right) \\
K_{31}u + K_{32}v + K_{33}w &= R^2 \rho_t \left(\frac{\partial^2 w}{\partial t^2} - 2 \frac{\partial v}{\partial t} - w \right)
\end{aligned} \quad (18)$$

In appendix-I, differential operators: $K_{11} + K_{12} + \dots + K_{33}$ are tabulated.

4. Wave propagation approach (WPA) for FG-CS

Here WPA is used to solve the CSs problem of differential equations in an efficient and comprehensive way. This method needs the axial modal approximates dependence on the characteristic function. The present analysis Zhang *et al.* (2002) is carried to examine the frequency spectrum of FG-CSs. Over the past several years vibration of shell and plate structures of various configurations and boundary conditions have been extensively studied (Wuite *et al.* 2005, Chi, and Chung, 2006). The present technique is very powerful for the prediction of vibration of shells.

$$\begin{aligned}
u(x, \theta, t) &= \alpha_m e^{-ik_m x} \sin(n\theta + \omega t) \\
v(x, \theta, t) &= \beta_m e^{-ik_m x} \cos(n\theta + \omega t) \\
w(x, \theta, t) &= \gamma_m e^{-ik_m x} \sin(n\theta + \omega t)
\end{aligned} \quad (19)$$

An eigenvector gives the shape of the three displacement components $\alpha_m, \beta_m, \gamma_m$ along the axis of the tube. The number of circumferential wave mode n and axial wave mode m demonstrate for modes of vibrations of a fluid-filled FG-CS. We classify the modes attached with each frequency into three types viz radial (bending), axial (longitudinal) and circumferential modes. On putting Eq (19) into Eq. (18) give up the following eigenvalue form:

$$\left\{ \begin{array}{ccc} L_{11} & L_{12} & L_{13} \\ L_{21} & L_{22} & L_{23} \\ L_{31} & L_{32} & L_{33} \end{array} \right\} + \left\{ \begin{array}{ccc} 1 & 0 & 0 \\ 0 & 1 & 0 \\ 0 & 0 & 1 \end{array} \right\} \rho_t \omega \left\{ \begin{array}{c} \alpha_m \\ \beta_m \\ \gamma_m \end{array} \right\} = 0 \quad (20)$$

Moreover, the Eq. (20) is written in eigenvalue form:

$$\{L_1 + L_2 \omega + L_3 \omega^2\} [x] = 0 \quad (21)$$

Here terms $L_{ij}(i, j=1,2,3)$ implicate geometrical and material quantities and are tabulated in the Appendix-II. From these values, the minimum absolute real value is chosen because six eigenvalues consists for its solution for the vibration of fluid-filled FG-CS.

5. Annexation of fluid term

The acoustic wave equation represents pressure of sound in fluid and this equation of motion describing fluid is given by

$$\frac{1}{r} \frac{\partial}{\partial r} \left(r \frac{\partial \phi}{\partial r} \right) + \frac{1}{r^2} \frac{\partial^2 \phi}{\partial \theta^2} + \frac{\partial^2 \phi}{\partial x^2} = \frac{1}{c^2} \frac{\partial^2 \phi}{\partial t^2} \tag{22}$$

where (x, θ, r) are the cylindrical coordinates and ϕ, t, c, r stands respectively, for acoustic pressure, time variable, fluid sound speeds and the axial coordinate adopted from the shell axis. The acoustic pressure expression for an immersed cylinder in a fluid that satisfied the acoustic wave Eq. (22), written in following form:

$$\phi = \phi_m \sin(n\theta) H_n^{(2)}(k_r r) \psi(x) \cos \omega t \tag{23}$$

where ϕ_m symbolizes the pressure amplitude, $H_n^{(2)}(k_r r)$ denotes the second kind of Hankel functions with order n . The radial and axial wave numbers k_r and k_x respectively linked by the vector equation, $k_r = (k_0 - k_x)^{1/2}$, where $k_0 = \frac{\omega}{c}$ is written for the acoustic wave number of the fluid. Here k_r has many values and depends on the variable k_x . In order to ensure that the sound field fulfills the suitable conditions of radiation and decay as $r \rightarrow \infty$, the branch that meets the condition $k_r = \sqrt{k_0 - k_x}$ for $k_0 \geq k_x$ and $k_r = -i\sqrt{k_x - k_0}$ for $k_0 < k_x$, is chosen. For the assurance of keeping fluid connection with shell wall, the radial displacement of the fluid must be equal to that at the boundary of the outer wall of shell and the fluid.

The coupling condition is applied and is written as:

$$-\left\{ 1 / (i\omega\phi_r) \right\} (\partial\phi / \partial r) |_{r=R} = (\partial w / \partial t) |_{r=R} \tag{24}$$

Subsequently the above condition has new form:

$$\phi_m = \left[\omega^2 \rho_f / k_r H_n^{(2)}(k_r R) \right] C_m \tag{25}$$

where ρ_f signifies the fluid density and the dot written upon the $H_n^{(2)}(k_r r)$ represents the differentiation w.r.t the argument $k_r R$. With the application of the coupling condition (29) along with the relation (25), the shell frequency of the submerged CSs is given by in matrix notation as:

$$\begin{pmatrix} L_{11} & L_{12} & L_{13} \\ L_{21} & L_{22} & L_{23} \\ L_{31} & L_{32} & L_{33} + FL \end{pmatrix} \begin{pmatrix} \alpha_m \\ \beta_m \\ \gamma_m \end{pmatrix} = \begin{pmatrix} 0 \\ 0 \\ 0 \end{pmatrix} \tag{26}$$

where $L_{ij}(i, j = 1, 2, 3)$ and FL defines the fluid loading term and is written as :

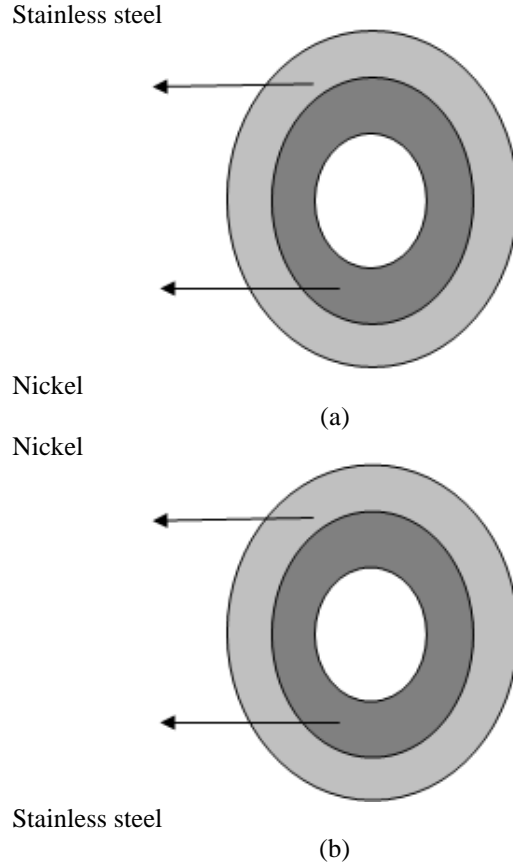


Fig. 1 FG-CSs (a) Type-I (b) Type-II

$$FL = \Omega^2 (\rho_f / \rho_s) (R/h) (k_r R)^{-1} \left[H_n^{(2)}(k_r R) / H_n^{(2)}(k_r R) \right] \tag{27}$$

When the fluid loaded term reduces to zero, the frequency equation fluid-filled cylindrical shells converts into that for the empty shell case.

6. Numerical results and discussion.

In this section, the versatile numerical technique WPA has been used in current study to investigate the vibration of fluid-filled FG-CS. For the convergence rate of CSs, the non-dimensional frequency enumerated in the current work, i.e., using WPA are happened to be in a good consistency along with the so-called exact results furnished by Loy *et al.* (1997), those were established by working out with the deformation theory provided in Table 1. The proposed model based on WPA can incorporate in order to accurately predict the acquired results of material data point. In Table 2, the coupled and uncouple frequency results are well matched those evaluated by Zhang *et al.* (2001) for different modal numbers for C-C shells. There is once again comparison of empty and fluid-filled CSs with Gonclaves *et al.* (2006) as shown in Table 3. The proposed model based on WPA can incorporate in order to accurately predict the acquired results of material data point.

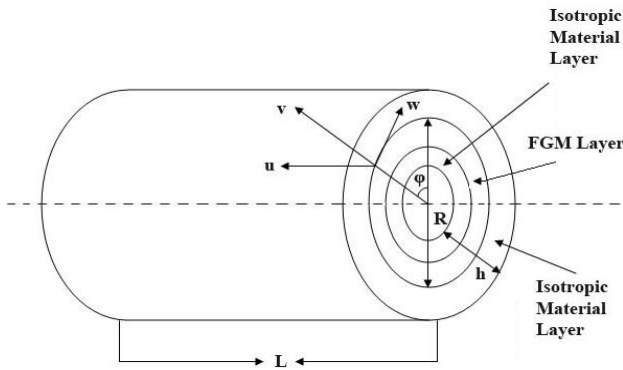


Fig. 2 Geometry of three layered shell

Table 1 Convergence of WPA frequencies (Loy *et al.* 1997)

Method	n				
	1	2	3	4	
C-C	Loy <i>et al.</i> (1997)	0.032885	0.01393	0.02267	0.04221
	Present	0.034878	0.01405	0.02272	0.04227
S-S	Loy <i>et al.</i> (1997)	0.016101	0.00938	0.02211	0.04209
	Present	0.016102	0.00938	0.02211	0.04227
C-S	Loy <i>et al.</i> (1997)	0.023974	0.00822	0.00584	0.00871
	Present	0.024721	0.00828	0.00585	0.00871

Table 2 Convergence of WPA frequencies (Zhang *et al.* 2001)

Method	Modal order (m, n)				
	(1,3)	(2,3)	(3,3)	(3,4)	
Coupled Frequency	Zhang <i>et al.</i> (2001)	8.94	10.64	14.66	19.96
	Present	8.90	10.62	14.59	19.85
Uncoupled Frequency	Zhang <i>et al.</i> (2001)	19.61	23.28	31.98	39.78
	Present	19.6	23.31	32.01	39.81

Table 3 Convergence of WPA frequencies (Gonclaves *et al.* 2006)

Method	n				
	8	9	10	11	
Empty cylindrical shell	Gonclaves <i>et al.</i> (2006)	280.940	288.71	318.4	363.33
	Present	279.145	287.54	317.43	362.87
Fluid-filled cylindrical shell	Gonclaves <i>et al.</i> (2006)	119.20	127.90	146.7	173.30
	Present	118.64	121.54	134.0	152.83

Table 4 Configuration of layers

Layers	Configuration	
	I	II
Inner layer (Iso)	$h/3$	$h/4$
Middle layer (FGM)	$h/3$	$h/2$
Outer layer (Iso)	$h/3$	$h/4$

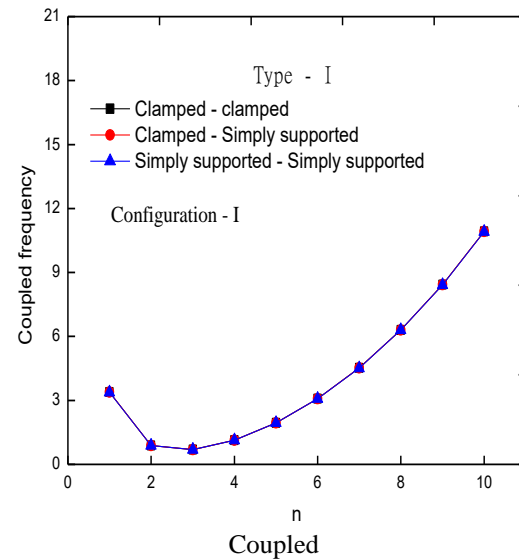
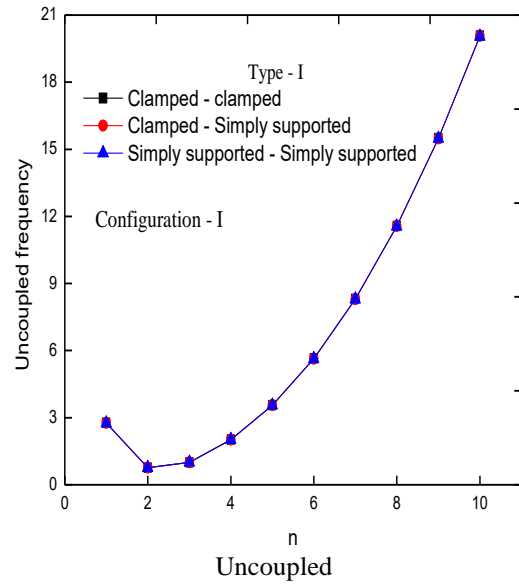


Fig. 3 Variation of uncoupled and coupled three layered S-S, C-S, C-C frequency versus (n) of configuration-I with Type-I for FG-CSs

6.1 Coupled vibration of three-layered FG-CSs

Since a FG-CS is composed of three layers having different thickness, which is presented in the Table 4. The inner and outer layer of configuration –I and- II is composed as $h/3$ and $h/4$ respectively, whereas for middle layer of same configuration is $h/3$ and $h/2$, respectively.

Fig. 3 plots the graph of uncoupled and coupled frequencies of fluid-filled FG-CSs with three different BCs S-S, C-S, C-C. The frequencies in this figure are drawn as configuration-I with Type-I versus wave mode (n). These variations of frequencies are drawn with three types of end conditions. In these Figs., the S-S are lower than that of C-C and C-S. For three conditions, frequency variations show different behavior with configuration -I. The frequencies are visible and decreases for these three boundary conditions for first three values (n = 1). These frequencies first increases and gain maximum value with the increase of

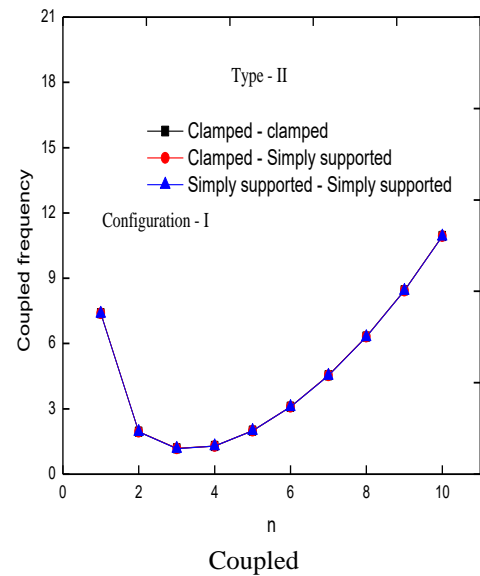
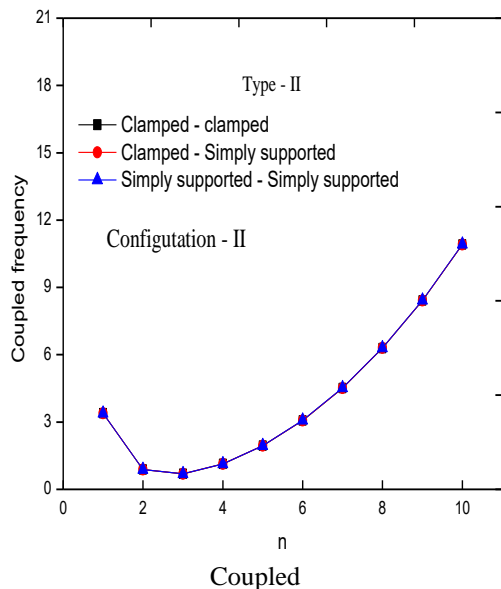
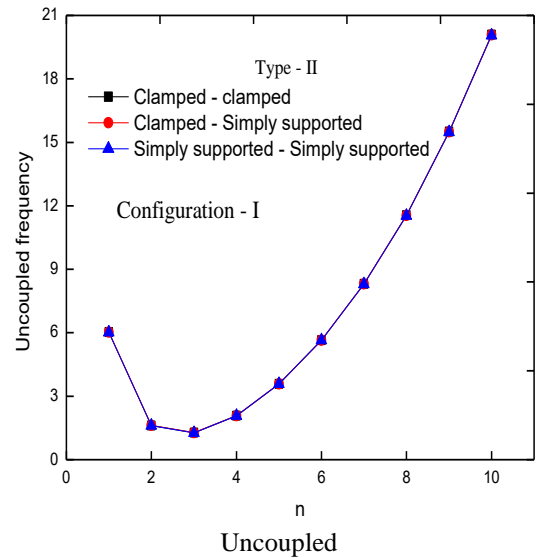
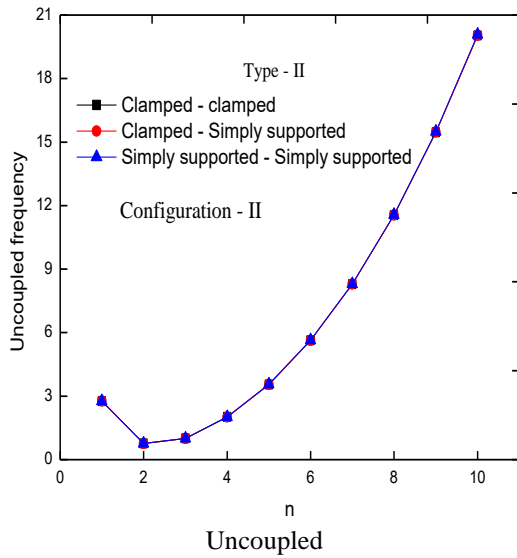


Fig. 4 Frequency variation of uncoupled and coupled three layered S-S, C-S, C-C edge conditions versus (n) of configuration-II with Type-I for FG-CSs

Fig. 5 Frequency variation of uncoupled and coupled three layered S-S, C-S, C-C versus (n) of configuration-I with Type-II for FG-CSs

circumferential wave mode. For clamped-clamped conditions, variations of frequencies are higher than that of other conditions. For $n = 4\sim 10$, a symmetrical behavior for natural frequencies is seen with proposed boundary conditions. The frequencies of C-S are sandwich with C-C and S-S conditions. It can be seen that coupled frequencies are smaller than that of uncoupled frequencies. It is due to the inducting of fluid term in the shell vibration. For other frequencies same phenomena is treated. Fig. 4 shows the frequency behavior of uncoupled and coupled frequencies for configuration-II with Type-I of FG-CSs with three different boundary conditions. Here the inner layer with thickness $h/2$ and thickness $h/4$ for outer layer. Due to combination of the layers frequency disordered as compared to the configuration-I with Type-I. In this case, the frequencies two times higher than that of configuration-I with Type-I. For higher values of n , frequencies get higher. For $n = 3$ for all boundary conditions, frequencies are lower

down. As shown by this figure, the boundary conditions C-C have the highest frequency curves. The frequencies are visible and decrease for these three boundary conditions for first three values. It is observed that uncoupled frequencies are higher than that of coupled frequencies. It is due to the inducting of fluid term in the shell vibration.

In Fig. 5, fundamental frequencies of fluid-filled CSs versus wave mode n with configuration-I and Type-II. The shell parameters $m = 1$, $L/R = 20$, $h/R = 0.002$ with three edge conditions. This frequency difference is regarded to changing the configuration of shell and this configuration change the flexural and membrane energy of the shell. The thickness of the middle layer is increased. The frequencies are visible and decreases for these three boundary conditions for first three values ($n = 1$). The frequency first increases and gain maximum value with the increase of circumferential wave mode. For clamped-clamped conditions, variations of frequencies are higher than that of other conditions.

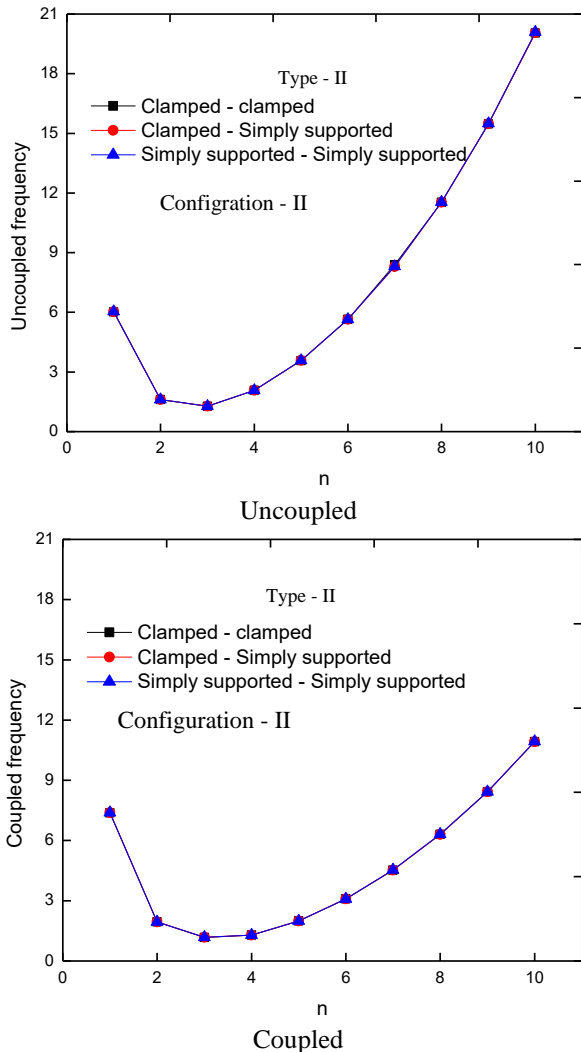


Fig. 6 Frequency variation of uncoupled three layered S-S, C-S, C-C versus (n) of configuration-II with Type-II for FG-CSs

In Fig. 6, fundamental frequencies of fluid-filled FG-CS are drawn versus wave mode n with configuration-II and Type-II. The frequencies are higher for higher values of n . The frequency first increases and gain maximum value with the increase of circumferential wave mode. For clamped-clamped conditions, variations of frequencies are higher than that of other conditions.

6. Conclusions

In this analytical study, coupled vibrations of fluid-filled functionally grade cylindrical shells have been investigated for the distribution of material composition of material with two categories of two types of material. Here the wave propagation approach has been applied to derive the shell frequency equation with fluid term. Hankel's functions of second kind are utilized to represent this phenomenon. The frequencies are higher for higher values of circumferential wave number. The frequency first increases and gain maximum value with the increase of circumferential wave

mode. For clamped-clamped conditions, variations of frequencies are higher than that of other conditions. It has been investigated that the frequencies lower down on implicating the fluid term. The uncoupled frequencies are higher than that of coupled frequencies. The shells are submerged in a fluid and terms describing fluid effects are added with the shell motion equations. The problem is formulated by applying the WPA and the shell fluid condition is annexed with the third equation of shell motion equations. The longitudinal modal displacement functions are assessed by characteristic beam ones meet end conditions applied at the shell edges. Stability of a cylindrical shell depends highly on these aspects of material. More the shell material sustains a load due to physical situations, the more the shell is stable. Any predicted fatigue due to burden of vibrations is evaded by estimating their dynamical aspects. An extension of present study can be done for investigating the rotating FG-shells with ring supports.

Acknowledgement

This research work was supported by the Deanship of Scientific Research at King Khalid University under grant number: RGP2/422/44.

References

- Amabili, M. (1999), "Vibration of circular tubes and shells filled and partially immersed in dense fluids", *J. Sound Vib.*, **221**(4), 567-585. <https://doi.org/10.1006/jsvi.1998.2050>
- Ansari, R., and Rouhi, H. (2015), "Nonlocal Flügge shell model for the axial buckling of single-walled Carbon nanotubes: An analytical approach", *Int. J. Nano Dimension*, **6**(5), 453-462. <https://doi.org/10.7508/IJND.2015.05.002>
- Arani, A.G., Kolahchi, R. and Esmailpour, M. (2016), "Nonlinear vibration analysis of piezoelectric plates reinforced with carbon nanotubes using DQM", *Smart. Struct. Syst.*, **18**(4), 787-800. <http://doi.org/10.12989/sss.2016.18.4.787>
- Arefi, M. and Zenkour, A.M. (2017), "Nonlinear and linear thermo-elastic analyses of a functionally graded spherical shell using the Lagrange strain tensor", *Smart. Struct. Syst.*, **19**, 33-38. <https://doi.org/10.12989/sss.2017.19.1.033>
- Arshad, S.H., Naeem, M.N. and Sultana, N. (2007). "Frequency analysis of functionally graded cylindrical shells with various volume fraction laws", *J. Mech. Eng. Sci.*, **221**, 1483-1495. <https://doi.org/10.1243/09544062JMES738>
- Asghar, S., Hussain, M. and Naeem, M. (2019), "Non-local effect on the vibration analysis of double walled carbon nanotubes based on Donnell shell theory", *Physica E*, **116**, 113726. <https://doi.org/10.1016/j.physe.2019.113726>
- Benmansour, D.L., Kaci, A., Bousahla, A.A., Heireche, H., Tounsi, A., Alwabli, A.S., Alhebshi, A.M., Al-ghmady, K. and Mahmoud, S.R. (2019), "The nano scale bending and dynamic properties of isolated protein microtubules based on modified strain gradient theory", *Adv. Nano Res.*, **7**(6), 443. <https://doi.org/10.12989/anr.2019.7.6.443>
- Chi, S.H. and Chung, Y.L. (2006), "Mechanical behavior of functionally graded material plates under transverse load-part II: numerical results", *Int. J. Solids Struct.*, **43**, 3657-3691. <https://doi.org/10.1016/j.ijsolstr.2005.04.010>
- Chung, H., Turula, P. Mulcahy, T.M. and Jendrzeczyk, J.A.

- (1981), "Analysis of cylindrical shell vibrating in a cylindrical fluid region", *Nuclear Eng. Des.*, **63**(1), 109-1012.
[https://doi.org/10.1016/0029-5493\(81\)90020-0](https://doi.org/10.1016/0029-5493(81)90020-0).
- Dong S.B. (1977), "A block-stodola eigen solution technique for large algebraic systems with non-symmetrical matrices", *Int. J. Numer. Method. Eng.*, **11**, 247.
<https://doi.org/10.1002/nme.1620110204>
- Ebrahimi, F., Dabbagh, A., Rabczuk, T. and Tornabene, F. (2019), "Analysis of propagation characteristics of elastic waves in heterogeneous nanobeams employing a new two-step porosity-dependent homogenization scheme", *Adv. Nano Res.*, **7**(2), 135.
<https://doi.org/10.12989/anr.2019.7.2.135>
- Eltaher, M.A., Almalki, T.A., Ahmed, K.I. and Almitani, K.H. (2019), "Characterization and behaviors of single walled carbon nanotube by equivalent-continuum mechanics approach", *Adv. Nano Res.*, **7**(1), 39. <https://doi.org/10.12989/anr.2019.7.1.039>
- Ergin, A. and Temarel, P. (2002), "Free vibration of a partially liquid-filled and submerged, horizontal cylindrical shell", *J. Sound Vib.*, **254**(5), 951-965.
<https://doi.org/10.1006/jsvi.2001.4139>
- Goncalves, P.B., Da Silva, F.M.A. and Prado, Z.J.G.N. (2006), "Transient stability of empty and fluid-filled cylindrical shells", *J. Brazil Soc. Mech. Sci. Eng.*, **28**(3), 331-333.
<http://doi.org/10.1590/S1678-58782006000300011>.
- He, J.H., Hou, W.F., Qie, N., Gepreel, K.A., Shirazi, A.H. and Mohammad-Sedighi, H. (2021), "Hamiltonian-based frequency-amplitude formulation for nonlinear oscillators", *Facta Univ. Series Mech. Eng.*, **19**(2), 199-208.
- He, J.H., Moatimid, G.M. and Zekry, M.H. (2022), "Forced nonlinear oscillator in a fractal space", *Facta Univ. Series Mech. Eng.*, **20**(1), 001-020.
- Jiang, J. and Olson, M.D. (1994), "Vibrational analysis of orthogonally stiffened cylindrical shells using super elements", *J. Sound Vib.*, **173**, 73-83.
<https://doi.org/10.1006/jsvi.1994.1218>
- Jweeg, M.J. and Alazzawy, W.I. (2009), "Free vibration Analysis solution for laminated truncated conical shells using high order theory", *Proceedings of the 6th College of Engineering - University of Baghdad*, **3**, 208-225.
- Jweeg, M.J. and Alazzawy, W.I. (2007), "A suggested analytical solution for laminated closed cylindrical shells using General Third Shell Theory (GTT)", *Al-Nahrain J. Eng. Sci.*, **10**(1), 11-26.
- Jweeg, M.J., Alazzawy, W.I. and Dep, M.E. (2010), "A study of free vibration and fatigue for cross-ply closed cylindrical shells using General Third shell Theory (GTT)", *J. Eng.*, **16**(6), 5170-5184.
- Koizumi, M. (1997), "FGM Activities in Japan", *Composites*.
- Loy, C.T., Lam, K.L. and Shu, C. (1997), "Analysis of cylindrical shells using generalized differential quadrature", *Shock Vib.*, **4**(3), 193-198. <https://doi.org/10.3233/SAV-1997>.
- Ma, H. (2022), "Simplified Hamiltonian-based frequency-amplitude formulation for nonlinear vibration systems", *Facta Univ. Series Mech. Eng.*, **20**(2), 445-455.
- Naeem, M.N., Ghamkhar, M., Arshad, S.H. and Shah, A.G. (2013), "Vibration analysis of submerged thin FGM cylindrical shells", *J. Mech. Sci. Technol.*, **27**(3), 649-656.
<http://10.1007/s12206-013-0119-6>
- Najafizadeh, M.M. and Isvandzibaei, M.R. (2007), "Vibration of (FGM) cylindrical shells based on higher order shear deformation plate theory with ring support", *Acta Mech.*, **191**, 75-91. <http://10.1007/s00707-006-0438-0>
- Sharma, P., Singh, R. and Hussain, M. (2019), "On modal analysis of axially functionally graded material beam under hygro-thermal effect", *Proceedings of the Institution of Mechanical Engineers, Part C: Journal of Mechanical Engineering Science*, **234**(5), 1085-1101.
<https://doi.org/10.1177/0954406219888234>
- Safaei, B., Khoda, F.H. and Fattahi, A.M. (2019), "Non-classical plate model for single-layered graphene sheet for axial buckling", *Adv. Nano Res.*, **7**, 265-275.
<https://doi.org/10.12989/anr.2019.7.4.265>
- Sewall, J.L. and Naumann, E.C. (1968), *An Experimental and Analytical Vibration Study of Thin Cylindrical Shells with and Without Longitudinal Stiffeners*, National Aeronautic and Space Administration, for sale by the Clearinghouse for Federal Scientific and Technical Information, Virginia, U.S.A.
- Shah, A.G., Mahmood, T. and Naeem, M.N. (2009), "Vibrations of FGM thin cylindrical shells with exponential volume fraction law", *Appl. Math. Mech.*, **30**(5), 607-615.
<https://doi.org/10.1007/s10483-009-0507-x>
- Shahsavari, D., Karami, B. and Janghorban, M. (2019), "Size-dependent vibration analysis of laminated composite plates" *Adv. Nano Res.*, **7**(5), 337-349.
<https://doi.org/10.12989/anr.2019.7.5.337>
- Sharma, C.B., Darvizeh, M. and Darvizeh, A. (1998), "Natural frequency response of vertical cantilever composite shells containing fluid", *Eng. Struct.*, **20**(8), 732-737.
[https://doi.org/10.1016/S0141-0296\(97\)00102-8](https://doi.org/10.1016/S0141-0296(97)00102-8)
- Sodel W. (1981), *Vibration of Shell and Plates*, Mechanical Engineering series, Marcel Dekker, New York, U.S.A.
- Sofiyev, A.H. and Avcar, M. (2010), "The stability of cylindrical shells containing an FGM layer subjected to axial load on the pasternak foundation", *Engineering*, **2**, 228-236.
<https://doi.org/10.4236/eng.2010.24033>
- Suresh, S. and Mortensen, A. (1997), "Functionally gradient metals and metal ceramic composites, Part 2: Thermo mechanical behavior", *Int. Mater.*, **42**, 85-116.
<https://doi.org/10.1179/imr.1995.40.6.239>
- Touloukian, Y.S. (1967), "Thermo physical properties of high temperature solid materials", Macmillan, New York, U.S.A.
- Wang, C.M., Swaddiwudhipong, S. and Tian, J. (1997), "Ritz method for vibration analysis of cylindrical shells with ring-stiffeners", *J. Eng. Mech.*, **123**, 134-143.
- Wang, C. and Lai, J.C.S. (2000), "Prediction of natural frequencies of finite length circular cylindrical shells", *Appl. Acoust.*, **59**(4), 385-400. [https://doi.org/10.1016/S0003-682X\(99\)00039-0](https://doi.org/10.1016/S0003-682X(99)00039-0)
- Wuite, J. and Adali, S. (2005), "Deflection and stress behavior of nanocomposite reinforced beams using a multiscale analysis", *Compos Struct*, **71**(3-4), 388-396.
<https://doi.org/10.1016/j.compstruct.2005.09.011>
- Xiang, Y., Ma, Y.F., Kitipornchai, S., Lau, C.W.H. (2002), "Exact solutions for vibration of cylindrical shells with intermediate ring supports", *Int. J. Mech. Sci.*, **44**(9), 1907-1924.
[https://doi.org/10.1016/S0020-7403\(02\)00071-1](https://doi.org/10.1016/S0020-7403(02)00071-1)
- Xuebin, L. (2008), "Study on free vibration analysis of circular cylindrical shells using wave propagation", *J. Sound Vib.*, **311**, 667-682. <https://doi.org/10.1016/j.jsv.2007.09.023>
- Zhang, X.M., Liu G.R. and Lam, K.Y. (2001), "Coupled vibration of fluid-filled cylindrical shells using the wave propagation approach", *Appl. Acoust.*, **62**, 229-243.
- Zhang, X.M. (2002), "Parametric analysis of frequency of rotating laminated composite cylindrical shells with the wave propagation approach", *Comput. Method Appl. Mech. Eng.*, **191**, 2057-2071. [https://doi.org/10.1016/S0045-7825\(01\)00368-1](https://doi.org/10.1016/S0045-7825(01)00368-1).

Appendix I

$$\begin{aligned}
 K_{11} &= A_{11} \frac{\partial^2}{\partial x^2} + \left(\frac{A_{66}}{R^2} + \rho_t \frac{\partial^2}{\partial \theta^2} \right) \\
 K_{12} &= \frac{(A_{12} + A_{66})}{R} \frac{\partial^2}{\partial x \partial \theta} + \frac{(B_{12} + 2B_{66})}{R^2} \frac{\partial^2}{\partial x \partial \theta} \\
 K_{13} &= \left(\frac{A_{12}}{R} - \rho_t R \right) \frac{\partial}{\partial x} - B_{11} \frac{\partial^3}{\partial x^3} - \frac{(B_{12} + 2B_{66})}{R^2} \frac{\partial^3}{\partial x \partial \theta^2} \\
 K_{21} &= \left(\frac{A_{12} + A_{66}}{R} + \frac{B_{12} + B_{66}}{R^2} + \rho_t R \right) \frac{\partial^2}{\partial x \partial \theta} \\
 K_{22} &= \left(A_{66} + \frac{3B_{66}}{R} + \frac{2D_{66}}{R^2} \right) \frac{\partial^2}{\partial x^2} + \left(\frac{A_{22}}{R^2} + \frac{2B_{22}}{R^3} + \frac{D_{22}}{R^4} \right) \frac{\partial^2}{\partial \theta^2} + \rho_t \\
 K_{23} &= \left(\frac{A_{22}}{R^2} + \frac{B_{22}}{R^3} \right) \frac{\partial}{\partial \theta} - \left(\frac{B_{22}}{R^3} + \frac{D_{22}}{R^4} \right) \frac{\partial^3}{\partial \theta^3} - \left(\frac{B_{12} + 2B_{66}}{R} + \frac{D_{12} + 2D_{66}}{R^2} \right) \frac{\partial^3}{\partial x^2 \partial \theta} - 2\rho_t \frac{\partial}{\partial t} \\
 K_{31} &= -\frac{A_{12}}{R} \frac{\partial}{\partial x} + B_{11} \frac{\partial^3}{\partial x^3} + \left(\frac{B_{12} + 2B_{66}}{R^2} \right) \frac{\partial^3}{\partial x \partial \theta^2} \\
 K_{32} &= -\left(\frac{A_{22}}{R^2} + \frac{B_{22}}{R^3} + \rho_t \right) \frac{\partial}{\partial \theta} + \left(\frac{B_{22}}{R^3} + \frac{D_{22}}{R^4} \right) \frac{\partial^3}{\partial \theta^3} + \left(\frac{B_{12} + 2B_{66}}{R} + \frac{D_{12} + 4D_{66}}{R^2} \right) \frac{\partial^3}{\partial x^2 \partial \theta} + 2\rho_t \frac{\partial}{\partial t} \\
 K_{33} &= -\frac{A_{22}}{R^2} + \rho_t + \frac{2B_{12}}{R} \frac{\partial^2}{\partial x^2} + \left(\frac{2B_{22}}{R^3} + \rho_t \right) \frac{\partial^2}{\partial \theta^2} - D_{11} \frac{\partial^4}{\partial x^4} - 2 \left(\frac{D_{12} + 2D_{66}}{R^2} \right) \frac{\partial^4}{\partial x^2 \partial \theta^2} - \frac{D_{22}}{R^4} \frac{\partial^4}{\partial \theta^4}
 \end{aligned}$$

Appendix II

$$\begin{aligned}
 L_{11} &= -k_m^2 A_{11} - n^2 \left(\frac{A_{66}}{R^2} + \rho_t \right) + \rho_t \omega^2 \\
 L_{12} &= -ink_m \left(\frac{A_{12} + A_{66}}{R} + \frac{B_{12} + 2B_{66}}{R^2} \right) \\
 L_{13} &= -ik_m^3 B_{11} - ik_m \left(\frac{A_{12}}{R} - \rho_t R \right) - in^2 k_m \left(\frac{B_{12} + 2B_{66}}{R^2} \right) \\
 L_{21} &= ink_m \left(\frac{A_{12} + A_{66}}{R} + \frac{B_{12} + B_{66}}{R^2} + \rho_t R \right) \\
 L_{22} &= -k_m^2 \left(A_{66} + \frac{3B_{66}}{R} + \frac{2D_{66}}{R^2} \right) - n^2 \left(\frac{A_{22}}{R^2} + \frac{2B_{22}}{R^3} + \frac{D_{22}}{R^4} \right) + \rho_t \rho_t \omega^2 \\
 L_{23} &= -n \left(\frac{A_{22}}{R^2} + \frac{B_{22}}{R^3} \right) - n^3 \left(\frac{B_{22}}{R^3} + \frac{D_{22}}{R^4} \right) - nk_m^2 \left(\frac{B_{12} + 2B_{66}}{R} + \frac{D_{12} + 2D_{66}}{R^2} \right) + 2\rho_t \omega \\
 L_{31} &= ik_m \frac{A_{12}}{R} + ik_m^3 B_{11} + in^2 k_m \left(\frac{B_{12} + 2B_{66}}{R^2} \right) \\
 L_{32} &= -n \left(\frac{A_{22}}{R^2} + \frac{B_{22}}{R^3} + \rho_t \right) - n^3 \left(\frac{B_{22}}{R^3} + \frac{D_{22}}{R^4} \right) - nk_m^2 \left(\frac{B_{12} + 2B_{66}}{R} + \frac{D_{12} + 4D_{66}}{R^2} \right) + 2\rho_t \omega \\
 L_{33} &= -\frac{A_{22}}{R^2} + \rho_t - k_m^2 \frac{2B_{12}}{R} - n^2 \left(\frac{2B_{22}}{R^3} + \rho_t \right) - k_m^4 D_{11} - 2n^2 k_m^2 \left(\frac{D_{12} + 2D_{66}}{R^2} \right) - n^4 \frac{D_{22}}{R^4}
 \end{aligned}$$